THE JOURNAL OF BIOLOGICAL CHEMISTRY
Vol. 280, No. 29, Issue of July 22, pp. 27155–27164, 2005

Printed in U.S.A.

Strong Effects of an Individual Water Molecule on the Rate of Light-driven Charge Separation in the *Rhodobacter sphaeroides* Reaction Center*

Received for publication, February 22, 2005, and in revised form, April 19, 2005
Published, JBC Papers in Press, May 20, 2005, DOI 10.1074/jbc.M501961200

Jane A. Potter‡§, Paul K. Fyfe‡¶, Dmitrij Frolov‖, Marion C. Wakeham‡, Rienk van Grondelle‖, Bruno Robert, and Michael R. Jones‡ ‡‡**

*From the ‡Department of Biochemistry, School of Medical Sciences, University of Bristol, University Walk, Bristol, BS8 1TD, United Kingdom, ‖Department of Physics and Astronomy, Free University of Amsterdam, De Boelelaan 1081, 1081 HV, Amsterdam, The Netherlands, and **Service de Biophysique des Fonctions Membranaires, Département de Biologie Joliot-Curie/CEA and URA 2096 CNRS, CEA Saclay, 91191 Gif-sur-Yvette, France*

The role of a water molecule (water A) located between the primary electron donor (P) and first electron acceptor bacteriochlorophyll (B_A) in the purple bacterial reaction center was investigated by mutation of glycine M203 to leucine (GM203L). The x-ray crystal structure of the GM203L reaction center shows that the new leucine residue packs in such a way that water A is sterically excluded from the complex, but the structure of the protein-cofactor system around the mutation site is largely undisturbed. The results of absorbance and resonance Raman spectroscopy were consistent with either the removal of a hydrogen bond interaction between water A and the keto carbonyl group of B_A or a change in the local electrostatic environment of this carbonyl group. Similarities in the spectroscopic properties and x-ray crystal structures of reaction centers with leucine and aspartic acid mutations at the M203 position suggested that the effects of a glycine to aspartic acid substitution at the M203 position can also be explained by steric exclusion of water A. In the GM203L mutant, loss of water A was accompanied by an ~8-fold slowing of the rate of decay of the primary donor excited state, indicating that the presence of water A is important for optimization of the rate of primary electron transfer. Possible functions of this water molecule are discussed, including a switching role in which the redox potential of the B_A acceptor is rapidly modulated in response to oxidation of the primary electron donor.

Reaction centers are integral membrane protein complexes that transduce the energy of sunlight into a biologically useful form. In the purple photosynthetic bacterium *Rhodobacter sphaeroides* the reaction center consists of three polypeptides, termed H, L, and M, that encase 10 cofactors. These are four bacteriochlorophylls (BChl),[1] two bacteriopheophytins (BPhe), two ubiquinones, a single photoprotective carotenoid, and a non-heme iron atom (Fig. 1*A*). The BChl, BPhe, and ubiquinone cofactors are arranged around an axis of pseudo 2-fold symmetry in two membrane-spanning branches (1–4). The complex also contains a large number of bound water molecules, some of which play functional roles, for example during the reduction and protonation of the Q_B ubiquinone (5, 6).

Light excitation of the reaction center triggers electron transfer across the membrane from a pair of excitonically coupled BChl molecules (P) to the Q_A ubiquinone (Fig. 1*A*, *arrows*) (see Refs. 5–11 for reviews). In the first step, an electron is passed from the lower energy singlet excited state of P (denoted P*) to the adjacent A-branch monomeric BChl (B_A), forming the $P^+B_A^-$ radical pair with a time constant of 3–5 ps at room temperature. The electron is then passed to the A-branch BPhe (H_A), forming the $P^+H_A^-$ radical pair with a time constant of 0.5–2 ps. The second of these reactions is more rapid than the first, with the result that the $P^+B_A^-$ radical pair is difficult to detect as a discrete intermediate as the electron is passed from P* to H_A. The electron is then transferred from H_A^- to Q_A with a time constant of around 200 ps.

The acetyl and keto carbonyl substituent groups that are conjugated to the π electron system of the BChl and BPhe cofactors provide an opportunity for the protein to exert significant effects on their biophysical properties. In the particular case of B_A the acetyl carbonyl group is free from hydrogen bond interactions, whereas the keto carbonyl group is adjacent to a buried water molecule (Fig. 1*B*); this is referred to in the remainder of this report as water A. This water molecule is also adjacent to residue His M202 that provides the axial ligand to the pentacoordinated magnesium of the P_B BChl (Fig. 1*B*), allowing a potential through-bond connection to be traced between the P dimer and B_A (Fig. 1*B*, *dotted lines*). The validity of this through-bond link is addressed under "Discussion."

The presence of water A was first proposed by Robert and Lutz in 1988 (12) on the basis of experiments that indicated that the keto carbonyl of B_A is either in a polar local environ-

* This work was supported by the Biotechnology and Biological Sciences Research Council of the United Kingdom (to J. A. P., P. K. F., M. C. W., and M. R. J.) and the Netherlands Organization for Scientific Research (NWO) via the Dutch Foundation for Earth and Life Sciences (to D. F. and R. v. G.). The costs of publication of this article were defrayed in part by the payment of page charges. This article must therefore be hereby marked "*advertisement*" in accordance with 18 U.S.C. Section 1734 solely to indicate this fact.

The atomic coordinates and structure factors (code 2BOZ) have been deposited in the Protein Data Bank, Research Collaboratory for Structural Bioinformatics, Rutgers University, New Brunswick, NJ (http://www.rcsb.org/).

§ Present address: Centre for Biomolecular Sciences, University of St Andrews, North Haugh, St Andrews, Fife, KY16 9ST, United Kingdom.

¶ Present address: Division of Biological Chemistry and Molecular Microbiology, Faculty of Life Sciences, University of Dundee, Nethergate, Dundee, DD1 4HN, United Kingdom.

‡‡ To whom correspondence should be addressed. Tel.: 44-117-9287571; Fax: 44-117-9288274; E-mail: m.r.jones@bristol.ac.uk.

[1] The abbreviations used are: BChl, bacteriochlorophyll; B_A, first electron acceptor; B*, accessory bacteriochlorophyll singlet excited state; BPhe, bacteriopheophytin; H_A, A-branch bacteriopheophytin; P, primary donor of electrons; P*, primary donor singlet excited state; Q_A, A-branch ubiquinone; Q_B, B-branch ubiquinone; SADS, species-associated difference spectra.

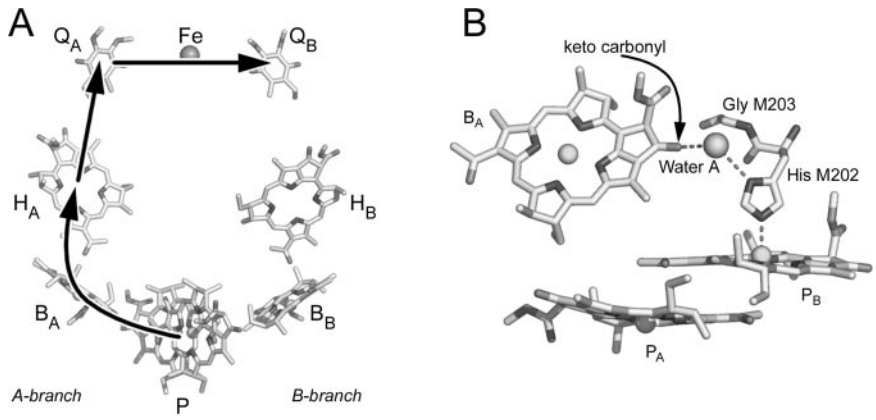

FIG. 1. **Structure of the wild type *R. sphaeroides* reaction center.** *A*, cofactor structure; the route of transmembrane electron transfer is indicated by the *arrows*. *B*, position of water A between the P dimer, His M202, and B_A. The *dotted lines* trace putative bond connections.

ment or that it is weakly hydrogen-bonded to the surrounding protein. An observed up-shift of the stretching frequency of this carbonyl group on oxidation of P further indicated that it becomes hydrogen-bonded when P is oxidized or that an existing weak hydrogen bond is strengthened (12). As a suitable hydrogen bond donor was not evident from available x-ray crystal structures of the *R. sphaeroides* reaction center, which at that time did not include water molecules, Robert and Lutz (12) proposed that the hydrogen bond donor could be a water molecule. This proposal was later confirmed following publication in 1994 of a new x-ray crystal structure of the complex that included water molecules (3, 4), and this water has been included in >80% of the structural models for wild-type or mutant reaction centers (that include waters) deposited in the Protein Data Bank (13) since that date.

Also adjacent to the keto carbonyl of B_A and water A is amino acid glycine M203 (Fig. 1*B*). In 1992, Williams *et al*. (14) introduced an aspartic acid at this position with a view to modulating the redox potential of B_A through the formation of a hydrogen bond with the keto carbonyl group (mutation denoted GM203D). By analogy with well documented effects of hydrogen bonding on the redox properties of P (15, 16), the addition of a hydrogen bond to the keto carbonyl of B_A could make this cofactor easier to reduce, lowering the free energy of the $P^+B_A^-$ state. In fact the rate of decay of the P* state was slowed in the GM203D mutant (14), suggesting a destabilization of B_A^- and an increase in the free energy of $P^+B_A^-$ state.

Two proposals have been made as to the origin of this destabilization. In the first, Czarnecki *et al*. (17) attributed it to a negative charge on the new aspartic acid residue. These experiments were carried out using the highly homologous *Rhodobacter capsulatus* reaction center, where the equivalent residue is glycine M201. In the second proposal, Fyfe *et al*. (18) determined the x-ray crystal structure of a mutant *R. sphaeroides* reaction center containing the GM203D change (Protein Data Bank entry 1E14), reporting that the new aspartic acid residue displaces water A but is in a poor position to donate an alternative hydrogen bond to the keto carbonyl of B_A. On the premise that this carbonyl group is hydrogen-bonded to water A in the wild-type reaction center, destabilization of B_A^- in the GM203D mutant was attributed to loss of a hydrogen bond because of steric exclusion of water A by the aspartic acid side chain.

In the present study, a new *R. sphaeroides* reaction center has been constructed in which glycine M203 is mutated to leucine (GM203L). The leucine side chain is similar in size and shape to aspartic acid but cannot carry a charge. The structure and functional properties of the GM203L reaction center reveal a strong influence of water A on the rate of primary charge separation.

MATERIALS AND METHODS

Construction of Mutant Strains—Single GM203D and GM203L mutations were constructed using the QuikChange mutagenesis kit (Stratagene). The template was plasmid pUCXB-1, which is a derivative of pUC19, containing a 1841-bp XbaI-BamHI restriction fragment encompassing *pufLM* (19). XbaI-BamHI restriction fragments containing the mutations were shuttled into expression vector pRKEH10D (20), which is a derivative of broad-host-range vector pRK415 containing a 6.25-kb EcoRI-HindIII fragment encoding *pufQLMX* (*i.e.* lacking the *pufBA* genes of the LH1 antenna complex). These derivatives of plasmid pRKEH10D were introduced into *R. sphaeroides* deletion strain DD13 (21) by conjugative transfer, as described previously (20). This produced transconjugant strains that had mutant reaction centers but lacked both types of light-harvesting complex.

Preparation of Intracytoplasmic Membranes and Purified Reaction Centers—Intracytoplasmic membranes for spectroscopic analysis were prepared using procedures described previously (22) from antenna-deficient *R. sphaeroides* cells that had been grown under semiaerobic conditions in the dark. For Raman spectroscopy, reaction centers were solubilized from membrane fragments suspended in 20 mM Tris/HCl (pH 8.0) by the addition of NaCl to 100 mM followed by lauryldimethylamine oxide to 0.3% and purified by two sequential passes through a DE52 anion exchange column, as described in detail elsewhere (19). Reaction centers for crystallization were further purified using Sepharose Q and Sephadex 200 columns (Amersham Biosciences) as described previously (19).

Reaction Center Crystallization and Data Analysis—Trigonal crystals, space group $P3_121$, were grown by sitting drop vapor diffusion as described previously (19). Briefly, well solutions containing 9 mg ml^{-1} of the GM203L reaction center, 0.09% v/v lauryldimethylamine oxide, 3.5% w/v heptane-1,2,3-triol, and 0.75 M potassium phosphate (pH 8.0) were equilibrated against a reservoir solution of 1.4 M potassium phosphate. Crystals appeared within 1–2 weeks and presented as prisms of variable size. The crystals had unit cell dimensions of $a = b = 138.6$ Å, $c = 185.3$ Å, $\alpha = \beta = 90°$, $\gamma = 120°$.

X-ray diffraction data were collected using cryo-cooled crystals and an ADSC Quantum 4 detector (Area Detector Systems Corp., Poway, CA) on beam-line 14.1 of the Daresbury Synchrotron Radiation Source, U.K. Crystals were prepared for cryo-cooling by sequential soaking in mother liquor containing increasing concentrations of glycerol to give a final concentration of 35%. The data were processed and scaled using HKL2000 (23). Molecular replacement was performed using AMORE (24) using the coordinates of the wild-type reaction center as the search model. Refinement was performed using restrained maximum likelihood refinement in REFMAC 5.0 (25). The collection and refinement statistics are given in Table I, and the structure has been deposited in the Protein Data Bank under accession code 2BOZ.

Spectroscopy—Room temperature absorbance spectra were recorded using a Beckman DU640 spectrophotometer, and 77 K absorbance spectra were recorded using a PerkinElmer Lamda35 spectrophotometer and an Oxford Instruments OptistatDN liquid nitrogen cryostat. In both cases sodium ascorbate and phenazine methosulfate were added to final concentrations of 1 mM and 25 μM, respectively, to ensure full reduction of the P BChls. Resonance Raman spectra were recorded at 77 K from samples of purified reaction centers as described recently (26). Femtosecond transient absorbance difference spectra were also recorded using antenna-deficient membranes as described in detail recently (27, 28). Excitation was at 795 nm, and spectra were fitted

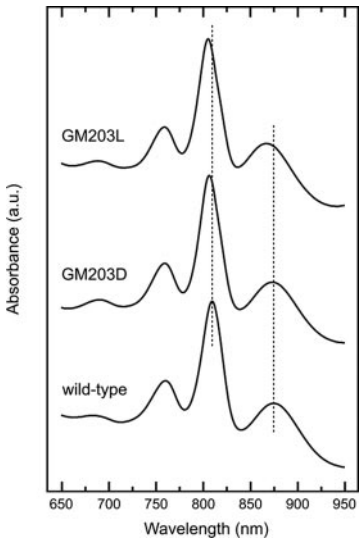

FIG. 2. **Room temperature absorbance spectra of membrane-bound reaction centers.** Spectra are offset for comparison, and *vertical dotted lines* indicate the maxima of the B and P Q_y absorbance bands in the wild-type reaction center.

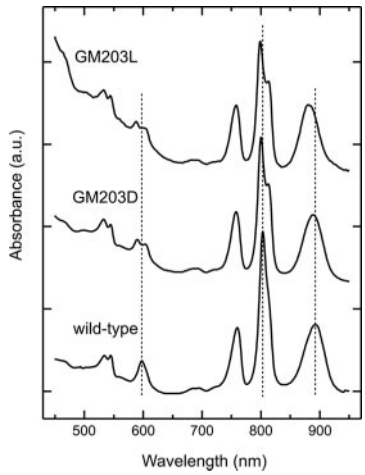

FIG. 3. **77 K absorbance spectra of purified reaction centers.** Spectra are offset for comparison.

globally with four components using an irreversible sequential model as described previously (29).

RESULTS

Absorbance Spectroscopy—Reaction centers with the mutations GM203D and GM203L were constructed as described under "Materials and Methods" and expressed in a background that lacks the LH1 and LH2 antenna complexes. Fig. 2 compares the Q_y region of the absorbance spectra of membrane-bound wild-type, GM203D and GM203L reaction centers. Neither mutation affected the position of the H Q_y band at 756 nm, which is attributed to the reaction center BPhes. However, both mutations produced a small blue-shift of the B Q_y band, which is attributed principally to the monomeric BChls. This band has an absorbance maximum at 805 nm in the membrane-bound wild-type reaction center and was shifted to 802 nm in the GM203D mutant and 801 nm in the GM203L mutant. A blue-shift of this band in the GM203D reaction center is consistent with previous reports of absorbance spectra at cryogenic temperatures (14, 18, 30, 31), suggesting an effect on B_A. Also consistent with previous findings from low temperature spectroscopy (18), the Q_y band of the P BChls showed a small blue-shift, from 868 to 866 nm, in the GM203D mutant. This band was further blue-shifted to 860 nm in the GM203L mutant.

To determine whether these absorbance changes were affected by detergent solubilization, absorbance spectra were also recorded for purified reaction centers at both room temperature (not shown) and 77 K (Fig. 3). This also gave the opportunity to examine the Q_x spectral region, which is distorted by carotenoid absorbance and membrane scatter in spectra of membrane-bound complexes. In the Q_y region the 77 K spectra showed the same trends as the room temperature spectra, with small blue-shifts of the B and P Q_y bands in the GM203D mutant (3 and 4 nm, respectively; Fig. 3) and somewhat larger shifts in the GM203L mutant (5 and 10 nm, respectively; Fig. 3). The shoulder on the red side of the B Q_y band in the 77 K spectrum of the wild-type complex was resolved as a discrete component at 812–813 nm in the spectra of the two mutants. In the Q_x region the BChls of the wild-type reaction center gave rise to an asymmetric absorbance band at 597 nm with a shoulder on the red side at ~605 nm. In the spectra of both mutants this band split into two components with maxima at 604 and 590 nm (for GM203D) or 588 nm (for GM203L). The result with the GM203D reaction center was consistent with previous reports on the effects of this mutation (14, 30, 32); the simplest interpretation of this change is that both GM203 mutations cause a blue-shift of the Q_x transition of B_A.

X-ray Crystallography—To compare the structural consequences of the GM203L and GM203D mutations, the x-ray crystal structure of the GM203L reaction center was determined to a resolution of 2.4 Å. Reaction centers were crystallized as described under "Materials and Methods," and diffraction data were collected from a single cryo-cooled crystal. Data collection and refinement statistics are shown in Table I. The structural model of the GM203L reaction center was compared with that of the wild-type complex determined previously (19). This comparison showed that there was excellent structural conservation throughout the bulk of the protein-cofactor system. Significant changes in structure were confined to the immediate environment of the M203 residue.

Modeling of the GM203 side chain and the surrounding area was carried out on the basis of omit maps. The initial round of refinement was performed with residues M201 to M205 replaced with alanine, with the exception of M203, which was maintained as a glycine. The side chains of these residues were then manually inserted into the resulting difference maps. The density for the side chain of M203 was continuous with the main chain and showed strong agreement with the insertion of a leucine. There was no evidence for the presence of a water molecule at or near the position expected for water A in the structure of the wild-type reaction center.

Fig. 4*B* shows a stereo view of the electron density corresponding to Leu M203 in the GM203L reaction center, and the fitted structural model. Fig. 4, *A* and *C*, shows approximately the same view of this region in the structures of the wild-type and FM197R/GM203D reaction centers, determined in previous work to resolutions of 2.6 and 2.7 Å, respectively (18, 19). In Fig. 4 (all panels), the B_A BChl is shown on the *left* and His M202 on the *right* above the P_B BChl. The Leu residue at the M203 position (Fig. 4*B*) occupied approximately the same position as Asp M203 in the GM203D mutant reaction center (Fig. 4*C*) and, as with this Asp residue, the Leu M203 residue occupied the space that accommodates water A in the structure of the wild-type reaction center (center view in Fig. 4*A*). These changes apart, the only other discernable alteration in structure was a small shift in the position of residue His M202, which had rotated away from the new Leu M203 by ~15–20 degrees around an axis defined approximately by the C–C bond (CG–CB) connecting carbon 4 of the imidazole ring to the beta carbon of the side chain. This rotation did not have any signif-

TABLE I
Crystallographic statistics for data collection and refinement

Parameter	GM203L reaction center
Collection statistics	
Resolution range	18.0–2.40 Å
No. of unique observations	80240
Completeness[a]	99.6% (97.6%)
Redundancy[a]	5.4 (3.4)
R_{merge}[b]	9.6%
Refinement statistics	
R_{cryst}[c]	17.4%
R_{free}[d]	19.7%
r.m.s.[e] bond distance deviation	0.018 Å
r.m.s. bond angle deviation	1.881°
Ramachandran plot, residues[f]	
Most favored areas	92.8%
Additionally allowed areas	6.6%
Generously allowed areas	0.6%
Disallowed areas	0.0%
Coordinate error[g]	0.17 Å
Model	
No. of protein residues	823
No. of cofactors	4 BChl, 2 BPhe, 2 Ubi, 1 Spo, 1 Fe
No. of waters	387
No. of detergents	4
No. of phosphates	2

[a] Figures within brackets refer to the statistics for the outer resolution shell (2.44–2.40 Å).

[b] $R_{merge} = \Sigma_h\Sigma_i|\langle I(h)\rangle - I(h)_i|/\Sigma_h\Sigma_i I(h)_i$, where $I(h)$ is the intensity of reflection h, Σ_h is the sum over all reflections, and Σ_i is the sum over all i measurements of reflection h.

[c] R_{cryst} is defined by $\Sigma||F_o| - |F_c||/\Sigma\ |F_o|$

[d] R_{free} was calculated with 5% reflections selected to be the same as in the refinement of the wild-type reaction center (19).

[e] r.m.s., root mean square.

[f] The Ramachandran plot was produced by Procheck, version 3.0 (65).

[g] Coordinate error was estimated by Cruickshank's diffraction-component precision index (DPI) (66).

icant effect on the length of the bond connecting the NE1 nitrogen of His M202 to the magnesium of P_B. This rotation was also seen in the structure of the GM203D/FM197R reaction center (Fig. 4*C*) and is considered again under "Discussion."

Two other aspects of the model of the GM203L reaction center are worth mention. First, the cardiolipin molecule reported in a number of publications (18, 33, 34–40) was not resolved, although density corresponding to the P_A phosphoryl group was observed and modeled as a phosphate ion (not shown). Factors that may affect the quality and completeness of the electron density corresponding to this cardiolipin molecule were discussed recently (41). Second, the Q_B ubiquinone was found at high occupancy in the so-called proximal binding site (not shown), with B-factors for the head group that were only very slightly higher than those of the surrounding protein. The average B-factor for the side chains of the 10 amino acids immediately surrounding the Q_B head group was 35.5, whereas the average B-factor for the quinone head group is 41.6. The quinone would be expected to show some elevation in B-factor values, as it has more conformational freedom than an amino acid bound within the polypeptide chain. The result suggests high occupancy of the Q_B site in the crystallized GM203L reaction center.

Resonance Raman Spectroscopy—Resonance Raman spectroscopy was used to examine the effects of the mutations on the adjacent keto carbonyl of B_A. The resonance Raman spectrum of ferricyanide-treated wild-type reaction centers at 77 K, excited at 800 nm, is shown in Fig. 5. As discussed previously (26), the resonance Raman spectrum of untreated or chemically reduced reaction centers is strongly distorted above 1100 cm^{-1} by fluorescence emission from P, but this emission band is lost when P is oxidized to P^+ by treatment with ferricyanide.

As has been described (26), the spectrum obtained with 800 nm excitation of ferricyanide-oxidized reaction centers comprises bands arising from B_A. Consistent with previous reports on R26-1 reaction centers (26) (within 2 cm^{-1}), the spectrum of the wild-type reaction center consisted of four main bands at 1584, 1612, 1659, and 1676 cm^{-1}. The last of these bands has been attributed to the keto carbonyl group of B_A, hydrogen-bonded to the adjacent water A. In the spectra of both mutants the 1584, 1612, and 1659 cm^{-1} bands were well conserved, but the 1676 cm^{-1} band appeared to have shifted to ~1700 cm^{-1} in the GM203D mutant and ~1704 cm^{-1} in the GM203L mutant (see *arrows* in Fig. 5). Possible origins of these up-shifts are considered under "Discussion."

Picosecond Time Scale Transient Absorbance Spectroscopy—The effects of the GM203L and GM203D single mutations on the kinetics of transmembrane electron transfer were investigated by picosecond time scale transient absorbance spectroscopy as described under "Materials and Methods." Absorbance difference spectra were obtained at varying time intervals after a 795-nm excitation pulse with a maximum delay time of 2–3 ns. Spectra recorded at several delay times are shown in Fig. 6, *A* and *B*, for the GM203D and GM203L mutants, respectively. The 795-nm pulse mainly excited B_A, with some excitation of B_B, causing a bleach around 800 nm in the spectrum of the GM203D mutant at early delay times (50 fs spectrum, Fig. 6*A*). Subsequent rapid excitation transfer from the monomeric BChls to the P BChl dimer caused a bleaching of the P band around 865 nm, concomitant with a loss of the bleach at 800 nm (1-ps spectrum, Fig. 6*A*). Stimulated emission on the red side of the bleach of the 865 nm P band was maximal at around 0.5 ps and subsequently decayed as electron transfer took place from P* to H_A (38-ps spectrum compared with 1-ps spectrum, Fig. 6*A*). A similar spectral evolution was observed for the GM203L mutant, but the bleach of the P band was somewhat blue-shifted, consistent with the shift of this band seen in the ground state absorbance spectrum (Fig. 2). The spectra were similar in general terms with spectra recorded previously for membrane-bound wild-type reaction centers (42, 43), with a bleach of the P Q_y band, the appearance and decay of P* stimulated emission on the red side of this bleach, and the appearance of an electrochromic blue-shift of the B Q_y band and an electrochromic red-shift of the H Q_y band. The most noticeable difference between the spectra in Fig. 6 and spectra recorded previously for the wild-type complex was a decrease in the relative magnitude of the band shift feature around 800 nm compared with that of the bleach of the P Q_y band. Possible reasons for this are considered under "Discussion."

A global analysis of the data was carried out using an irreversible sequential model (*i.e.* $1 \rightarrow 2 \rightarrow 3 \rightarrow$). Four spectrally and temporally distinct components were needed to describe the data, and the species-associated difference spectra (SADS) of these components are shown in Fig. 7, *A–D* and *E–H*, for the GM203D and GM203L mutants, respectively. Also shown for comparison are SADS determined for membrane-bound wild-type reaction centers (Fig. 7, *I–L*). In all three cases the first component was attributed to the short-lived excited states of the accessory BChls (B*), formed by the 795 nm excitation pulse, with a lifetime of 160–200 fs (Fig. 7, *A*, *E,* and *I*). This evolved into a state with a spectrum that was characteristic of P*, which in turn had a lifetime of 20 ps in the GM203D mutant (Fig. 7*B*), 42 ps in the GM203L mutant (Fig. 7*F*), and 5 ps in the wild-type complex (Fig. 7*J*). The latter lifetime was similar to that described previously for membrane-bound wild-type *R. sphaeroides* reaction centers (4.5–4.8 ps) (42, 43).

The third state was assigned to $P^+H_A^-$ (Fig. 7, *C*, *G*, and *K*). In the GM203D mutant (Fig. 7*C*) this state decayed with a lifetime of 180 ps, similar to the 200-ps lifetime obtained for the

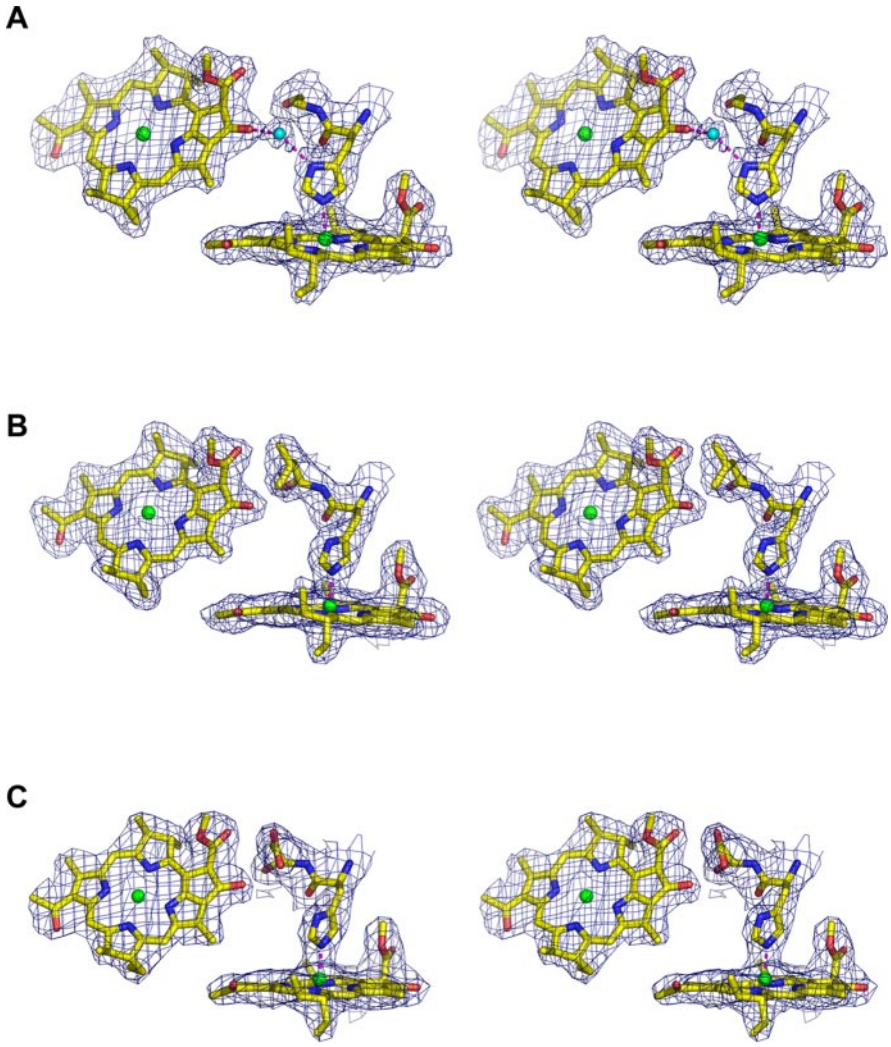

FIG. 4. **Stereo views of the $2mF_o - DF_c$ electron density map and fitted structures.** *A*, wild-type reaction center (19). *B*, GM203L mutant (present work). *C*, GM203D/FM197R reaction center (18). In all cases the view is the same as for Fig. 1*B* and shows the B_A and P_B BChls, His M202, the M203 residue, and water A (for the wild-type complex).

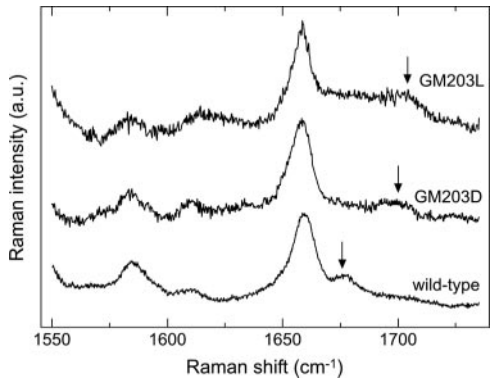

FIG. 5. **Resonance Raman spectra (1550–1735 cm^{-1}) of ferricyanide-treated purified reaction centers at 77 K, excited at 800 nm.** Straight-line base lines were subtracted from the original spectra.

wild type complex (Fig. 7*K* and Refs. 42 and 43), but in the GM203L mutant (Fig. 7*g*) this lifetime was ~600 ps. The final state was assigned to $P^+Q_A^-$ (Fig. 7, *D*, *G*, and *L*) and had a lifetime that was infinite on the time scale of the measurement. As expected from the time-resolved spectra, the magnitude of the differential signal due to the electrochromic blue-shift of the B Q_y band was strongly suppressed in the spectra of the $P^+H_A^-$ and $P^+Q_A^-$ states, with the negative, red-most lobe having an amplitude that was only around 20% of that of the neighboring bleach of the P Q_y band. In comparison, in SADS for the $P^+H_A^-$ and $P^+Q_A^-$ states in the wild-type reaction center (Fig. 7, *K* and *L*, and Refs. 42 and 43), this negative lobe had an amplitude of 65–80% of that of the bleach of the P Q_y band.

To summarize, both M203 mutations brought about a slowing in the rate of decay of the P* state, the strongest effect being seen in the GM203L reaction center; this mutation also seemed to affect the rate of electron transfer from H_A^- to Q_A. In addition, the relative magnitude of the electrochromic blue-shift of the B Q_y band was diminished by a factor of roughly 3-fold in both mutants.

DISCUSSION

Interactions of the B_A BChl with the Protein-Cofactor-Solvent Matrix—The widely accepted view of charge separation in the purple bacterial reaction center is that progression along each step in the reaction sequence, $P^* \rightarrow P^+B_A^- \rightarrow P^+H_A^- \rightarrow P^+Q_A^-$, is accompanied by a small drop in free energy. To achieve these drops, BPhe and quinone are used as the electron acceptors for the second and third steps, and all of the cofactors also engage in interactions with the surrounding the protein-cofactor matrix that fine-tune their electrochemical potential for oxidation or reduction. The most detailed study of the mechanism(s) of this fine-tuning has been made with the primary donor, BChls, and particular attention has been drawn to the role of the conjugated keto and acetyl carbonyl groups in engaging in hydrogen bond (15, 16, 44) and/or, in the case of the acetyl groups, charge-dipole interactions with amino acids in the surrounding protein (45).

Achievement of an appropriate free energy for the $P^+B_A^-$

state involves modulation of the oxidation potential of P and the reduction potential of B_A. In contrast to the P BChls, relatively little is known about the significance of the interactions that the acetyl and keto carbonyl groups of B_A make with the protein environment, and there is some disagreement as to what these interactions are. The acetyl group is agreed to be free from hydrogen bond interactions, its immediate environment being made up of atoms of the neighboring H_A and P_B cofactors and aromatic amino acids Phe L146, Phe L97, and Tyr L128. Turning to the keto carbonyl, the majority of structural models of the wild-type *R. sphaeroides* reaction center determined from x-ray diffraction data during the last 10 years include a water molecule located within hydrogen bond distance (~2.9 Å) of the keto carbonyl group of B_A (water A). A second water molecule is similarly located close to the keto carbonyl group of B_B (referred to below as water B). The same arrangement is seen in the structure of the *Blastochloris viridis* (formerly *Rhodopseudomonas viridis*) reaction center (46–48), and in the reaction center from *Thermochromatium tepidum* (49). In *R. sphaeroides*, water A is within hydrogen bond distance of a number of polar groups, including the keto oxygen of B_A (2.9 Å), a second water (2.9 Å), the ND nitrogen of the side chain of His M202 (2.9 Å), the backbone carbonyl oxygens of Phe M197 (3.5 Å) and Phe M196 (3.8 Å). Distances in brackets are taken from the 1QOV structure (33, 50). Assuming that it is hydrogen bonded to the adjacent carbonyl group of B_A, water A therefore allows a through-bond connection to be traced between the P dimer and B_A via His M202 as illustrated in Fig. 1*B*.

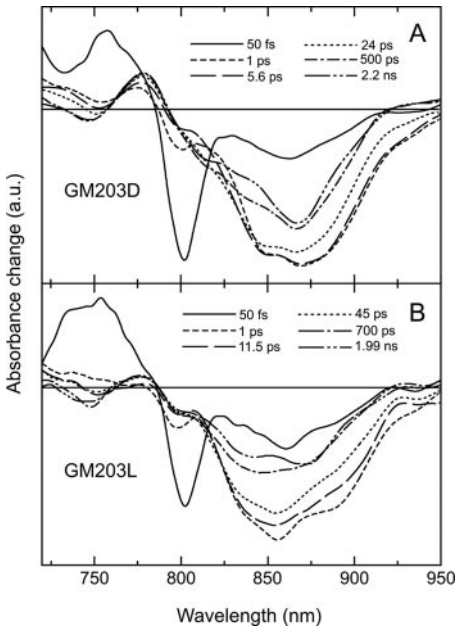

FIG. 6. **Transient absorbance difference spectra obtained at various times after excitation with a 60-fs excitation pulse centered at 795 nm.** *A*, GM203D membrane-bound reaction centers. *B*, GM203L membrane-bound reaction centers.

Effects of Mutagenesis of Residue Gly M203—The data summarized in Fig. 4 demonstrate that mutation of residue M203 to either Leu or Asp causes steric exclusion of water A. This change in structure is accompanied by a strong decrease in the rate of primary charge separation (Figs. 6 and 7). This is particularly the case for the GM203L mutant, where the 8-fold slowing in the rate of P* decay is one of the largest effects on the kinetics of primary electron transfer reported to date for a single mutation (that does not change the cofactor composition of the reaction center). The x-ray crystal structure of the GM203L complex shows that the mutation has very limited effects on the structure of the reaction center.

To understand the source of these effects it is useful to compare data obtained with the GM203L and GM203D complexes with previous observations. The ~3-fold slowing of the rate of P* decay reported previously for purified *R. sphaeroides* GM203D reaction centers (14), from 3.4 ps (in the wild-type) to 9.4 ps, is broadly consistent with the ~4-fold slowing reported here for membrane-bound reaction centers (from 4.8 to 20 ps). Primary electron transfer has been reported to be somewhat slower in membrane-bound reaction centers than in purified complexes (42, 51). The decrease in the rate of primary electron transfer caused by the GM203D mutation has been attributed to an increase in the free energy of the $P^+B_A^-$ state. In purified *R. capsulatus* reaction centers the equivalent Gly M201 to Asp mutation has been shown to increase the yield of B-branch electron transfer (52), which would also be consistent with an increase in the free energy of the $P^+B_A^-$ state.

As discussed above, two alternative explanations for the effects of the GM203D mutation have been put forward, a charge-dipole interaction exerted by a charged Asp side chain that destabilizes the adjacent B_A anion (17) and the removal of a water molecule that, in the wild-type complex, stabilizes the B_A anion (18). Either of these would raise the free energy of the

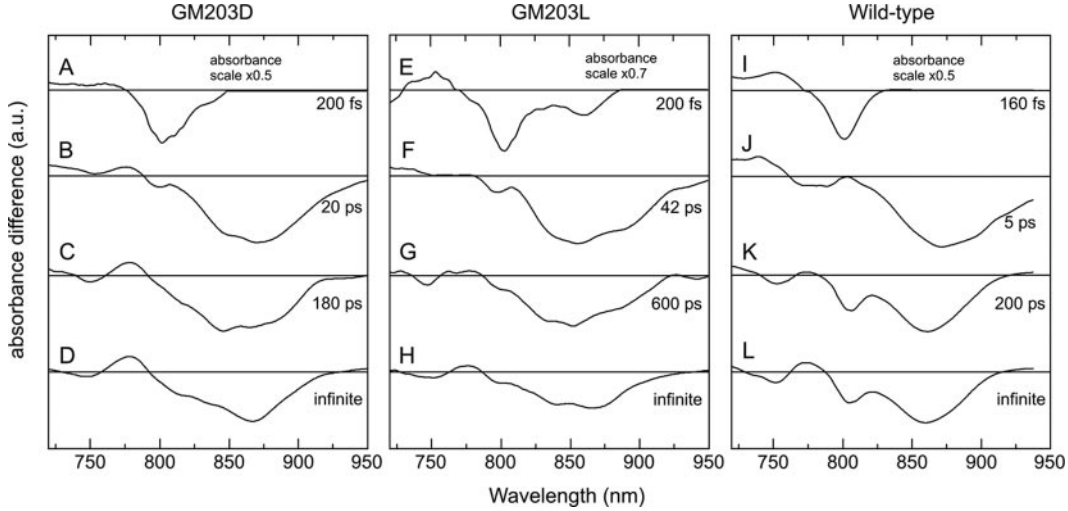

FIG. 7. **SADS and associated lifetimes derived from a global analysis of transient absorbance spectra obtained after 795 nm excitation.** *A–D*, GM203D membrane-bound reaction centers. *E–H*, GM203L membrane-bound reaction centers. *I–L*, wild-type membrane-bound reaction centers. For the purposes of comparison, spectra *A*, *E*, and *I* were multiplied by factors of 0.5, 0.7, and 0.5, respectively.

$P^+B_A^-$ state (or lower the free energy of a $B_A^+H_A^-$ state, as has recently also been proposed for the GM203D mutation (53)). In the present study, we have shown that mutation of Gly M203 to either Asp or Leu removed water A, blue-shifted both the Q_x and Q_y transitions of B_A, slowed the rate of P* decay, and up-shifted the stretching frequency of the keto carbonyl of B_A (to ~1700 and 1704 cm^{-1}, respectively). The fact that the Asp and Leu mutations had similar effects argues against proposals that the Asp M203 residue exerts its effects through being charged (17) and provides strong support for modulation of the properties of the B_A cofactor through exclusion of water A (18). A further point worth noting is that computational studies have predicted that a negative charge near the keto carbonyl of a BChl should cause a blue-shift of the Q_x absorbance and a red-shift of the Q_y absorbance (32, 54, 55) in contrast to the observed effects of the GM203D mutation (Figs. 2 and 3). Again, this argues against the Asp M203 residue being charged.

How do B_A and Water A Interact in the Wild-type Reaction Center?—The x-ray crystal structure of the wild-type reaction center shows that water A is within hydrogen bond distance of the keto carbonyl of B_A (3, 4). However, at the resolutions currently available for the purple bacterial reaction center, the presence of a hydrogen bond between the two can be inferred only from the crystallographic data.

Based on data from resonance Raman spectroscopy, Robert and Lutz (12) have proposed that in neutral reaction centers, the keto carbonyl of B_A could be involved in a weak hydrogen bond with water A. They noted however that the observed 1689 cm^{-1} stretching frequency of this group could also be explained if its local environment has a high permittivity. In a later study Czarnecki *et al*. (17) concluded that the 1689 cm^{-1} frequency of this carbonyl group is too high to be consistent with the presence of a hydrogen bond, and therefore it must be free from hydrogen bond interactions with the surrounding protein.

Key to the question of whether water A could be hydrogen-bonded to the keto carbonyl of B_A in neutral reaction centers is the upper limit of the stretching frequency of a keto carbonyl group that is free from hydrogen bond interactions with the surrounding protein. There is no simple answer to this question, as the frequency of this group is also affected by the local dielectric environment. For instance, the stretching frequency of the keto carbonyl of BPhe *a* and Ni-BPhe *a* (*i.e.* nickel-substituted BPhe *a*) in different solvents has been shown to vary over a range of 12 cm^{-1}, with the highest values being obtained in the solvents with the lowest dielectric constant (56). Considering photosynthetic proteins, the keto carbonyls of the P BChls in the *R. sphaeroides* reaction center have stretching frequencies at 1679 cm^{-1} (P_B) and 1691 cm^{-1} (P_A), but according to the x-ray crystal structure, neither group is hydrogen-bonded to the surrounding protein. The 12 cm^{-1} difference between these groups has been ascribed to a difference in their dielectric environments (with the keto group of P_B in a region of relatively high dielectric constant (57)). In mutant LH2 antenna complexes from *R. sphaeroides*, the stretching frequency of the free keto carbonyl of the B800 monomeric BChls has been reported to be in the range 1689–1702 cm^{-1} (58), the precise value probably depending on the dielectric properties of its environment in a particular mutant complex.

In the present report, the stretching frequency of the B_A keto group was observed at 1704 cm^{-1} (Fig. 5), which seems likely to correspond to the upper limit for the stretching frequency of a keto carbonyl. In (neutral) wild-type reaction centers, the observed down-shift relative to this value is 15 cm^{-1}, which could be consistent either with the presence of a weak hydrogen bond donated by a polar water A or with a difference in the permittivity of the protein environment of the carbonyl group due to the presence of water A. It is therefore not possible to determine whether water A exerts its influence through a hydrogen bonding or permittivity effect. In a similar vein, the effects of the GM203L and GM203D mutations on the absorbance spectrum of the reaction center are consistent both with the expected effects of removal of a hydrogen bond interaction between the keto carbonyl of B_A and water A (58–61) and with the predicted effects of changing the polarity of the environment of the BChl (55, 58, 62) Nevertheless, irrespective of the mechanism involved, it is clear that water A influences the stretching frequency of the keto carbonyl group of B_A. In the *oxidized* reaction center, the observed 1675 cm^{-1} frequency provides unambiguous evidence for the presence of a hydrogen bond between water A and the keto carbonyl of B_A (12, 26). This is observed both when the reaction center is chemically oxidized to form P^+, as in the present work (Fig. 5), or when it is photo-oxidized to form $P^+Q_A^-$. Oxidation of P is therefore either accompanied by the formation of a weak hydrogen bond (of around 1.9 $kcal.mol^{-1}$) or by an approximate doubling in the strength of an existing bond.

In the GM203D reaction center, where water A is displaced by a polar Asp side chain, the stretching frequency of the B_A keto carbonyl is at 1700 cm^{-1} (18). Although, as argued above, it is unlikely that this Asp residue is charged, when neutral this residue bears a weak permanent dipole (63). As a result the presence of an apolar Leu or a weakly polar Asp at position M203 should elicit different effects on the properties of B_A, which was indeed observed. Compared with an Asp, the presence an apolar Leu induced (*a*) slightly larger blue-shifts of the Q_x and Q_y electronic transitions of B_A, (*b*) a larger slowing of the rate of primary charge separation, and (*c*) a larger up-shift of the stretching frequency of the keto carbonyl group of B_A. These observations suggest that changes in local permittivity play a significant role in determining the properties of the M203 mutants.

As a final point, previous discussions of the influence of water A on the kinetics of primary electron transfer have focused on the effects of this water molecule on the redox properties of B_A and the free energy change for the $P^* \rightarrow P^+B_A^-$ reaction. However, it is conceivable that the removal of water A could also slow the rate of P* decay through a change in the reorganization energy for the reaction, given that water A is a potentially mobile and polar molecule located between B_A and the P BChls. We also cannot exclude the possibility that structural changes in the GM203L and GM203D mutants, such as the observed rotation of His M202 for example (Fig. 4, *B* and *C* compared with *A*), could change the electronic structure of the P BChls, which might also have an effect on the characteristics of the primary charge separation reaction. It would be interesting, for example, to examine any changes in spin density distribution between the two halves of the P dimer caused by loss of water A and rotation of His M202. Changes in the midpoint potential of the P/P^+ redox couple (E_m P/P^+) could also produce a slowing of the rate of primary charge separation and contribute to a difference between the Asp and Leu mutants, but preliminary measurements indicate that neither mutation had a significant effect on E_m P/P^+,[2] which is in good agreement with previous reports on the GM203D mutation (14).

Conservation of the Protein-Cofactor Environment of Water A—Given the very high degree of structural conservation across the reaction centers of purple bacteria, one indicator of

[2] C. McKibbin, J. A. Potter, P. K. Fyfe, and M. R. Jones, unpublished observations.

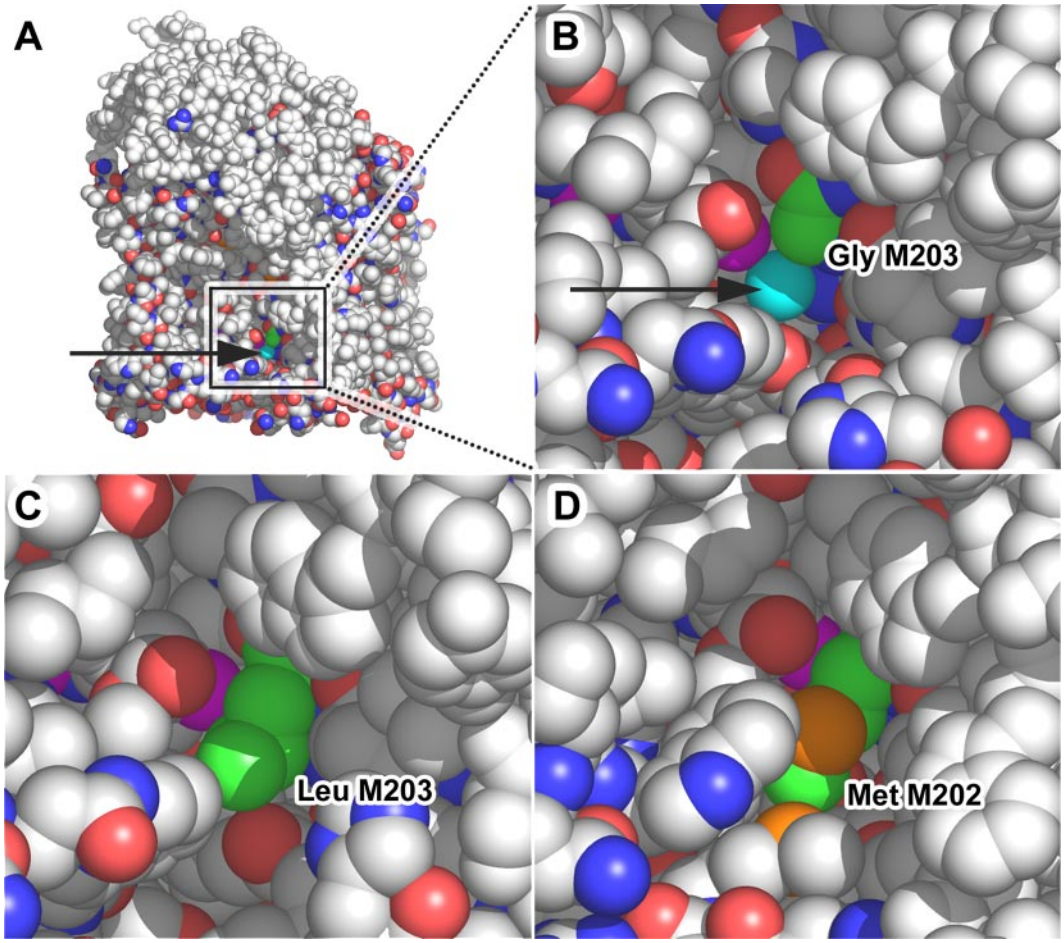

FIG. 8. **The location of water A.** *A*, space-filled representation of the *R. sphaeroides* reaction center viewed approximately parallel to the plane of the membrane. *B*, zoomed view of the region around residue Gly M203 and water A. *C* and *D*, equivalent views of this region of the GM203L mutant reaction center (*C*) and the reaction center from *T. tepidum* (*D*), respectively. The L- and M-polypeptides are shown in cpk (Corey-Pauling-Koltun) color scheme, with the H-polypeptide highlighted in *all white*. The keto oxygen of B_A is highlighted in *magenta* and water A in *cyan* (indicated by the *arrow* in *A* and *B*). The M203 (*A–C*) and M202 (*D*) residues are shown in cpk colors but with *green* carbon atoms.

the possible functional importance of water A as a modulator of the rate of charge separation could be the extent to which its protein environment is conserved. Examination of an alignment of 46 sequences for the PufM polypeptide (64), shows that a Gly residue at the M203 position occurs in only six sequences, including *R. sphaeroides*, *R. capsulatus*, and *B. viridis*. This residue is an Ala in 19 sequences, Met in 17, Val in one, and Cys in three; thus the extremely small Gly side chain is not a conserved feature of the complex, although it happens to be found in the three most heavily studied reaction centers. In the *T. tepidum* reaction center, where there is also crystallographic information, this residue is a Met (numbered M202 in this bacterium) (49).

Fig. 8*A* shows a space-filled view of the intramembrane surface of the *R. sphaeroides* reaction center, with the backbone of Gly M203 highlighted in *green*, water A highlighted in *cyan*, and the keto oxygen of B_A highlighted in *magenta*. The M203 residue and water A are located close to the intramembrane surface of the reaction center and are not buried deep in the protein interior. Fig. 8*B* shows an enlarged view of the region around the M203 residue. When Gly M203 is replaced by Leu (Fig. 8*C*), the residue packs in such a way that the side chain points downward and inward in the view presented in Fig. 8*C*, and water A is displaced. Inspection of the structure shows that the Leu residue is of an appropriate size to fit into the cavity left by exclusion of water A. This is also the case for an Asp residue at the M203 position (not shown). In contrast, the x-ray crystal structure of the *T. tepidum* reaction center shows that a larger Met residue at this position packs in such a way that water A is retained (Fig. 8*D*), with the longer Met side chain pointing downward and outward from the complex in the view presented in Fig. 8*D*. Water A is buried underneath the Met side chain. As a result, there does not seem to be any *a priori* reason to believe that water A is not a conserved structural feature because the adjacent Gly M203 is not conserved. As demonstrated by the *T. tepidum* reaction center (Fig. 8*D*), a bulkier side chain than Gly can be accommodated without displacing water A, by pointing the side chain outwards from the complex. As to why Asp and Leu pack in the way seen in the x-ray structures of the GM203D and GM203L mutants, it may simply be that these residues are just the right size to fit into the water A pocket without leaving too much empty space.

The x-ray crystal structures of the *R. sphaeroides*, *R. viridis*, and *T. tepidum* reaction centers also contain a water molecule (water B) positioned within hydrogen bonding distance of the keto carbonyl of the B_B BChl (*i.e.* on the B-branch of cofactors in a symmetrical position to water A). In the *R. sphaeroides* reaction center the symmetry-related residue to Gly M203 is Met L174, which adopts a conformation similar to Met M202 in *T. tepidum*, pointing outward from the complex. Residue Met L174 is conserved as Met in all but one of the 49 aligned sequences of the L polypeptide from purple photosynthetic bacteria, where it is a Cys (50). It therefore seems likely that water B is also a conserved structural feature of purple bacterial reaction centers, a point that will be re-examined below.

Why Water as a Hydrogen Bond Donor?—The results de-

scribed above for the wild-type and GM203L reaction centers provide strong evidence that water A forms a hydrogen bond interaction with B_A when P is oxidized, and the presence of this hydrogen bond is important for ensuring that primary electron transfer is rapid. Removal of this water causes a pronounced slowing of primary electron transfer. The choice of water as the hydrogen bond donor may be because the hydrogen-bonding amino acid residues are either too large to fit into the cavity adjacent to the keto carbonyl of B_A, or as in the case of an Asp residue, they adopt a poor geometry for hydrogen bonding once fitted into this cavity (18). However, another relevant factor may be the potential for water A to simultaneously hydrogen bond with the ND nitrogen of His M202, providing a direct through-bond connection between the primary donor BChls and B_A. This would not be likely if Gly M203 were replaced by His for example, as modeling studies indicate that if the ND nitrogen was in suitable position to interact with the keto of B_A, the NE nitrogen would not be a suitable position to interact with His M202.[3] Likewise, an amino acid side chain capable of undergoing only one hydrogen bond interaction could interact with the keto carbonyl of B_A, but the putative connecting interaction with His M202 and the P BChls would be lost.

The possibility of this through-bond connection between the primary electron donor and acceptor is intriguing, and its significance remains to be explored. A recent study involving excitation of GM203L reaction centers and deuterated wild-type reaction centers with 18-fs excitation pulses at 90 K has shown that water A has a significant influence on the dynamics of P* decay and on the population of the $P^+B_A^-$ and $P^+H_A^-$ states that are the products of charge separation.[4] This finding underscores the importance of water A for the primary charge separation reaction. One possible interpretation of these data is that this putative through-bond connection is involved in modulating the properties of B_A in response to photo-oxidation of P. Certainly it is evident from the present study that the electrochromic band-shift of the accessory BChls is strongly attenuated when water A is removed, and the $\sim$12 cm^{-1} downshift of the stretching frequency of the keto carbonyl of B_A is lost. These observations point to a desensitization of B_A to the change in the redox state of P following photoexcitation, and a possible role for water A in dynamically stabilizing B_A^- in response to oxidation of P. Such a stabilization would switch the protein-cofactor system into a state that favors fast charge separation. In the GM203L mutant, where water A is absent, the system is locked into a state where charge separation is relatively slow. It would be interesting to see if modulation of the properties of B_A by water A would be preserved if the connection between water A and the M202 residue were to be severed by mutation of the latter to a residue that can donate a ligand to the P_B BChl but not simultaneously donate a hydrogen bond to water A.

Finally, it is relevant to ask why a symmetry-related water molecule is found adjacent to the keto carbonyl of the B_B BChl. As discussed above, it is likely that water B is also a conserved feature of the purple bacterial reaction center, adding to the structural symmetry of a protein-cofactor system that nevertheless shows a very strong functional asymmetry; this arrangement is rather curious given the supposed exclusive use of the A-branch for transmembrane electron transfer. A much discussed idea is that the free energy of the potential $P^+B_B^-$ radical pair state is higher that that of the $P^+B_A^-$ state, and this energetic inequivalence ensures that almost all transmembrane electron transfer occurs along the A-branch. The structural factors that dictate this energetic inequivalence are not fully understood, but it would seem logical that a simple way to make $P^+B_B^-$ higher in energy than $P^+B_A^-$ would be to replace water B with a hydrophobic side chain, removing the possibility of hydrogen bond or charge-dipole interactions that could stabilize B_B^-. However, this does not appear to have happened during the evolution of the purple bacterial reaction center. The GM203L mutation described in this report points toward how the structural and functional effects of removing water B could be examined, by replacing Met L174 (the symmetry-related residue to Gly M203) with Leu, and experiments to this end are under way.

[3] P. K. Fyfe and M. R. Jones, unpublished observations.

[4] A. G. Yakovlev, M. R. Jones, J. A. Potter, P. K. Fyfe, L. G. Vasilieva, A. Ya. Shkuropatov, and V. A. Shuvalov, submitted for publication.

REFERENCES

1. Allen, J. P., Feher, G., Yeates, T. O., Komiya, H., and Rees, D. C. (1987) *Proc. Natl. Acad. Sci. U. S. A.* **84,** 5730–5734
2. Chang, C.-H., El-Kabbani, O., Tiede, D., Norris, J., and Schiffer, M. (1991) *Biochemistry* **30,** 5352–5360
3. Ermler, U., Fritzsch, G., Buchanan, S. K., and Michel, H. (1994) *Structure* **2,** 925–936
4. Ermler, U., Michel, H., and Schiffer, M. (1994) *J. Bioenerg. Biomembr.* **26,** 5–15
5. Okamura, M. Y., Paddock, M. L., Graige, M. S., and Feher, G. (2000) *Biochim. Biophys. Acta* **1458,** 148–163
6. Wraight, C. A. (2004) *Front. Biosci.* **9,** 309–337
7. Parson, W. W. (1991) in *Chlorophylls* (Scheer, H., ed) pp. 1153–1180, CRC Press, Boca Raton, FL
8. Woodbury, N. W., and Allen, J. P. (1995) in *Anoxygenic Photosynthetic Bacteria* (Blankenship, R. E., Madigan, M. T., and Bauer, C. E., eds) pp. 527–557, Kluwer Academic Publishers, The Netherlands
9. Parson, W. W. (1996) in *Protein Electron Transfer* (Bendall, D. S., ed) pp. 125–160, BIOS Scientific Publishers, Oxford
10. Hoff, A. J., and Deisenhofer, J. (1997) *Phys. Rep.* **287,** 2–247
11. Van Brederode, M. E., and Jones, M. R. (2000) in *Enzyme-Catalysed Electron and Radical Transfer* (Scrutton, N. S., and Holzenburg, A., eds) pp. 621–676, Kluwer Academic/Plenum Publishers, New York
12. Robert, B., and Lutz, M. (1988) *Biochemistry* **27,** 5108–5114
13. Berman, H. M., Westbrook, J., Feng, Z., Gilliland, G., Bhat, T. N., Weissig, H., Shindyalov, I. N., and Bourne, P. E. (2000) *Nucleic Acids Res.* **28** 235–242
14. Williams, J. C., Alden, R. G., Murchison, H. A., Peloquin, J. M., Woodbury, N. W., and Allen, J. P. (1992) *Biochemistry* **31,** 11029–11037
15. Allen, J. P., and Williams, J. C. (1995) *J. Bioenerg. Biomembr.* **27,** 275–283
16. Ivancich, A., Artz, K., Williams, J. C., Allen, J. P., and Mattioli, T. A. (1998) *Biochemistry* **37,** 11812–11820
17. Czarnecki, K., Kirmaier, C., Holten, D., and Bocian, D. F. (1999) *J. Phys. Chem. A Mol. Spectrosc. Kinet. Environ. Gen. Theory* **103,** 2235–2246
18. Fyfe, P. K., Ridge, J. P., McAuley, K. E., Cogdell, R. J., Isaacs, N. W., and Jones, M. R. (2000) *Biochemistry* **39,** 5953–5960
19. McAuley-Hecht, K. E., Fyfe, P. K., Ridge, J. P., Prince, S. M., Hunter, C. N., Isaacs, N. W., Cogdell, R. J., and Jones, M. R. (1998) *Biochemistry* **37,** 4740–4750
20. Jones, M. R., Visschers, R. W., van Grondelle, R., and Hunter, C. N. (1992) *Biochemistry* **31,** 4458–4465
21. Jones, M. R., Fowler, G. J. S., Gibson, L. C. D., Grief, G. G., Olsen, J. D., Crielaard, W., and Hunter, C. N. (1992) *Mol. Microbiol.* **6,** 1173–1184
22. Jones, M. R., Heer-Dawson, M., Mattioli, T. A., Hunter, C. N., and Robert, B. (1994) *FEBS Lett.* **339,** 18–24
23. Otwinowski, Z., and Minor, W. (1997) *Methods Enzymol.* **276,** 307–326
24. Navaza, J. (1994) *Acta Crystallogr. Sect. A* **50,** 157–163
25. Murshudov, G. N., Vagin, A. A., and Dodson, E. J. (1997) *Acta Crystallogr. Sect. D* **53,** 240–253
26. Frolov, D., Gall, A., Lutz, M., and Robert, B. (2002) *J. Phys. Chem. A Mol. Spectrosc. Kinet. Environ. Gen. Theory* **106,** 3605–3613
27. Wakeham, M. C., Frolov, D., Fyfe, P. K., van Grondelle, R., and Jones, M. R. (2003) *Biochim. Biophys. Acta* **1607,** 53–63
28. Gradinaru, C. C., van Stokkum, I. H. M., Pascal, A. A., van Grondelle, R., and van Amerongen, H. (2000) *J. Phys. Chem. B Condens. Matter Mater. Surf. Interfaces Biophys.* **104,** 9330–9342
29. van Stokkum, I. H. M., Scherer, T., Brouwer, A. M., and Verhoeven, J. W. (1994) *J. Phys. Chem.* **98,** 852–866
30. Kirmaier, C., Weems, D., and Holten, D. (1999) *Biochemistry* **38,** 11516–11530
31. Vos, M. H., Rischel, C., Breton, J., Martin, J.-L., Ridge, J. P., and Jones, M. R. (1998) *Photosynth. Res.* **55,** 181–187
32. Heller, B. A., Holten, D., and Kirmaier, C. (1996) *Biochemistry* **35,** 15418–15427
33. McAuley, K. E., Fyfe, P. K., Ridge, J. P., Isaacs, N. W., Cogdell, R. J., and Jones, M. R. (1999) *Proc. Natl. Acad. Sci. U. S. A.* **96,** 14706–14711
34. Camara-Artigas, A., Magee, C. L., Williams, J. C., and Allen, J. P. (2001) *Acta Crystallogr. Sect. D* **57,** 1281–1286
35. Pokkuluri, P. R., Laible, P. D., Deng, Y. L., Wong, T. N., Hanson, D. K., and Schiffer, M. (2002) *Biochemistry* **41,** 5998–6007
36. Camara-Artigas, A., Brune, D., and Allen, J. P. (2002) *Proc. Natl. Acad. Sci. U. S. A.* **99,** 11055–11060
37. Camara-Artigas, A., Magee, C., Goetsch, A., and Allen J. P. (2002) *Photosynth. Res.* **74,** 87–93
38. Katona, G., Andreasson, U., Landau, E. M., Andreasson, L. E., and Neutze, R. (2003) *J. Mol. Biol.* **331,** 681–692
39. Roszak, A. W., McKendrick, K., Gardiner, A. T., Mitchell, I. A., Isaacs, N. W.,

Cogdell, R. J., Hashimoto, H., and Frank, H. A. (2004) *Structure* **12,** 765–773
40. Xu, Q., Axelrod, H. L., Abresch, E. C., and Paddock, M. L. (2004) *Structure* **12,** 703–715
41. Jones, M. R., Fyfe, P. K., Roszak, A. W., Isaacs, N. W., and Cogdell, R. J. (2002) *Biochim. Biophys. Acta* **1565,** 206–214
42. Beekman, L. M. P., Visschers, R. W., Monshouwer, R., Heer-Dawson, M., Mattioli, T. A., McGlynn, P., Hunter, C. N., Robert, B., van Stokkum, I. H. M., van Grondelle, R., and Jones, M. R. (1995) *Biochemistry* **34,** 14712–14721
43. Beekman, L. M. P., van Stokkum, I. H. M., Monshouwer, R., Rijnders, A. J., McGlynn, P., Visschers, R. W., Jones, M. R., and van Grondelle, R. (1996) *J. Phys. Chem.* **100,** 7256–7268
44. Mattioli, T. A., Lin, X., Allen, J. P., and Williams, J. C. (1995) *Biochemistry* **34,** 6142–6152
45. Spiedel, D., Jones, M. R., and Robert, B. (2002) *FEBS Lett.* **527,** 171–175
46. Deisenhofer, J., Epp, O., Sinning, I., and Michel, H. (1995) *J. Mol. Biol.* **246,** 429–457
47. Lancaster, C. R. D., and Michel, H. (1997) *Structure* ***5***, 1339–1359
48. Lancaster, C. R. D., and Michel, H. (1999) *J. Mol. Biol.* **286,** 883–898
49. Nogi, T., Fathir, I., Kobayashi, M., Nozawa, T., and Miki, K. (2000) *Proc. Natl. Acad. Sci. U. S. A.* **97,** 13561–13566
50. McAuley, K. E., Fyfe, P. K., Ridge, J. P., Cogdell, R. J., Isaacs, N. W., and Jones, M. R. (2000) *Biochemistry* **39,** 15032–15043
51. Schmidt, S., Arlt, T., Hamm, P., Lauterwasser, C., Finkele, U., Drews, G., and Zinth, W. (1993) *Biochim. Biophys. Acta* **1144***,* 385–390
52. Heller, B. A., Holten, D., and Kirmaier, C. (1995) *Science* **269,** 940–945
53. Treynor, T. P., Yoshina-Ishii, C., and Boxer, S. G. (2004) *J. Phys. Chem. B Condens. Matter Mater. Surf. Interfaces Biophys.* **108,** 13523–13535
54. Eccles, J., and Honig, B. (1983) *Proc. Natl. Acad. Sci. U. S. A.* **80,** 4959–4962
55. Hanson, L. K., Fajer, J., Thompson, M. A., and Zerner, M. C. (1987) *J. Am. Chem. Soc.* **109,** 4728–4730
56. Lapouge, K., Naveke, A., Sturgis, J. N., Hartwich, G., Renaud, D., Simonin, I., Lutz, M., Scheer, H., and Robert, B. (1998) *J. Raman Spectrosc.* **29,** 977–981
57. Mattioli, T. A., Hoffman, A., Robert, B., Schrader, B., and Lutz, M. (1991) *Biochemistry* **30,** 4648–4654
58. Gall, A., Fowler, G. J. S., Hunter, C. N., and Robert, B. (1997) *Biochemistry* **36,** 16282–16287
59. Thompson, M. A., Zerner, M. C., and Fajer, J. (1991) *J. Phys. Chem.* **95,** 5693–5700
60. Bylina, E. J., Kirmaier, C., McDowell, L. M., Holten, D., and Youvan, D. C. (1988) *Nature* **336,** 182–184
61. Kirmaier, C., Laporte, L., Schenck, C. C., and Holten, D. (1995) *J. Phys. Chem.* **99,** 8903–8909
62. Braun, P., Vegh, A. P., von Jan, A., Strohmann, B., Hunter, C. N., Robert, B., and Scheer, H. (2003) *Biochim. Biophys. Acta* **1607,** 19–26
63. Sandberg, L., and Edholm, O. (2001) *J. Phys. Chem.* **105,** 273–281
64. Wakeham, M. C. (2004) *Inactive Branch Electron Transfer in the Purple Bacterial Reaction Center.* Ph.D. thesis, University of Bristol
65. Laskowski, R. A., MacArthur, W. W., Moss, D. S., and Thornton, J. M. (1993) *J. Appl. Crystallogr.* **26,** 283–291
66. Cruickshank, D. W. J. (1999) *Acta Crystallogr. Sect. D* **55,** 583–601